Interaction-energy functional for lattice density functional theory: Applications to one-, two-, and three-dimensional Hubbard models

R. López-Sandoval

Instituto Potosino de Investigación Científica y Tecnológica, Camino a la presa San José 2055, 78216 San Luis Potosí, México

G. M. Pastor

Laboratoire de Physique Quantique, Centre National de la Recherche Scientifique, Université Paul Sabatier, 31062 Toulouse, France

The Hubbard model is investigated in the framework of lattice density functional theory (LDFT). The single-particle density matrix γ_{ij} with respect to the lattice sites is considered as the basic variable of the many-body problem. A new approximation to the interaction-energy functional $W[\gamma]$ is proposed which is based on its scaling properties and which recovers exactly the limit of strong electron correlations at half-band filling. In this way, a more accurate description of W is obtained throughout the domain of representability of γ_{ij}, including the crossover from weak to strong correlations. As examples of applications results are given for the ground-state energy, charge-excitation gap, and charge susceptibility of the Hubbard model in one-, two-, and three-dimensional lattices. The performance of the method is demonstrated by comparison with available exact solutions, with numerical calculations, and with LDFT using a simpler dimer ansatz for W. Goals and limitations of the different approximations are discussed.

I. INTRODUCTION

Density functional theory (DFT) provides a rigorous framework for studying the physics of the many-body problem.[1–4] The fundamental concept behind DFT is to replace the conventional dynamical variables that completely define a many-particle state (e.g., the wave function in a quantum mechanical problem, or the particle positions and momenta in a classical system) by considering the particle-density distribution $\rho(\mathbf{r})$ as the basic variable. For this purpose the energy E of the system is expressed as a functional of $\rho(\mathbf{r})$ separating the various energy terms in two main groups. The first one contains the contributions that depend explicitly on the problem under study, which result from the coupling between $\rho(\mathbf{r})$ and the external fields $V_{ext}(\mathbf{r})$. The second one concerns the intrinsic energy of the many-particle system, namely, the kinetic energy T and the interaction energy W of the particles. These terms are universal functionals of $\rho(\mathbf{r})$ in the sense that they are independent of the problem under study. While the general functional dependence of $T[\rho]$ and $W[\rho]$ is not known explicitly, they can be formally expressed as the result of integrating out the microscopic degrees of freedom. In the case of ground-state electronic properties, this is achieved by imposing that $T[\rho]$ and $W[\rho]$ correspond to the minimum possible value of $T+W$ for a given $\rho(\mathbf{r})$.[3–5] These basic notions have general validity and are therefore relevant to a wide variety of situations which may have very different physical origins.

In the present paper the concepts of DFT are applied to investigate the physics of strongly correlated electrons in a narrow energy band. The theoretical description of these systems is usually based on lattice Hamiltonians such as Anderson,[6] Hubbard,[7] Pariser–Parr–Pople (PPP),[8] and related models which focus on the most relevant electron dynamics at low energies.[9–12] The study of many-body lattice models in the framework of DFT seems particularly interest-

ing from various perspectives. On the one side, a detailed understanding of the electronic properties in the strongly correlated limit constitutes an important theoretical challenge. Exact results are rare or numerically very demanding and a variety of elaborate many-body techniques are specifically developed for their study. Therefore, a density functional approach with an appropriate ansatz for W should be a useful alternative tool for investigating at least some aspects of this complex problem. On the other side, one would like to extend the range of applicability of DFT to strongly correlated phenomena, like the separation of charge and spin degrees of freedom or the correlation induced localization, where conventional local density approximations or generalized gradient approximations are known to fail systematically. Moreover, the development of DFT on a lattice constitutes an intrinsically inhomogeneous approach, which provides a true alternative to methods relying on the homogeneous electron gas. In this context, investigations on many-body models should open new insights into the properties of the interaction-energy functional that could also be useful for future extensions to more realistic Hamiltonians and first principles calculations.

In past years, a number of density functional studies of lattice models have been performed concerning in particular the determination of band gaps in semiconductors,[13] the role of off-diagonal elements of the density matrix and the non-interacting v representability in strongly correlated systems,[14] or the development of energy functionals of the density matrix with applications to Hubbard and Anderson models.[15] In previous papers we have formulated a lattice density functional theory (LDFT) of many-body models by considering the density matrix γ_{ij} with respect to the lattice sites i and j as the fundamental variable.[16–18] The interaction energy W of the Hubbard model has been calculated exactly as a function of γ_{ij} for various periodic lattices having $\gamma_{ij} = \gamma_{12}$ for nearest neighbors (NNs) i and j. On this basis, a

simple general approximation to $W(\gamma_{12})$ has been proposed which derives from exact dimer results, the scaling properties of W, and known limits. Using this ansatz, several ground-state properties of one-dimensional (1D) and two-dimensional (2D) systems have been obtained in good agreement with available exact solutions and accurate numerical calculations.[17] In addition, applications to dimerized chains provided us with systematic results for the ground-state energy and charge excitation gap of the 1D Hubbard model as a function of hopping alternation and Coulomb repulsion, including the crossover from weak to strong correlations.[18] LDFT therefore appears as an efficient method of determining the electronic properties of many-body lattice models, thus encouraging further developments and applications.

The main purpose of this paper is to present a new approximation to the interaction-energy functional $W[\gamma]$ of the Hubbard Hamiltonian and to apply it to determine several electronic properties of this model in the framework of LDFT. In Sec. II the basic formulation of LDFT is briefly reviewed. Different approximations to the interaction-energy functional are presented and discussed in Sec. III. First, we analyze the properties of a previously proposed dimer ansatz[17] and discuss its goals and limitations by comparison with known exact results. Some shortcomings of this functional in the limit of strong correlations at half-band filling are pointed out. In order to overcome them, we propose a new approximation based on the scaling properties of W, which recovers the correct behavior in the limit of strong interactions. In this way a more accurate description of the dependence on γ_{ij} in different dimensions and lattice structures is obtained. The following sections are mainly concerned with applications to 1D, 2D, and 3D Hubbard models. Results for the ground-state energy, charge-excitation gap, and charge susceptibility are presented in Secs. IV, V, and VI, respectively. Comparison is made with the simpler dimer ansatz and with exact analytical or numerical solutions, whenever available, in order to quantify the accuracy of the different approximations. Finally, Sec. VII summarizes the conclusions and points out some perspectives of future developments.

II. DENSITY-FUNCTIONAL THEORY OF LATTICE MODELS

In order to be explicit we focus on the Hubbard model which is expected to capture the main physics of lattice fermions in a narrow energy band. The Hamiltonian[7]

$$H = \sum_{\langle i,j \rangle \sigma} t_{ij} \hat{c}_{i\sigma}^\dagger \hat{c}_{j\sigma} + U \sum_i \hat{n}_{i\downarrow} \hat{n}_{i\uparrow}, \qquad (1)$$

includes nearest neighbor (NN) hoppings t_{ij}, and on-site interactions given by U ($\hat{n}_{i\sigma} = \hat{c}_{i\sigma}^\dagger \hat{c}_{i\sigma}$). The hopping integrals t_{ij} are defined by the lattice structure and by the range of the single-particle hybridizations (typically, $t_{ij} = -t < 0$ for NN ij). They specify the system under study and thus play the role given in conventional DFT to the external potential $V_{\mathrm{ext}}(\mathbf{r})$. Consequently, the basic variable in LDFT is the single-particle density matrix γ_{ij}. The situation is similar to

the density-matrix functional theory proposed by Gilbert for the study of nonlocal pseudopotentials,[19] since the hoppings are nonlocal in the sites. A formulation of DFT on a lattice in terms of the diagonal γ_{ii} alone is possible only if one restricts oneself to models with constant t_{ij} for $i \neq j$. In this case the functional $W[\gamma_{ii}]$ depends on the values of t_{ij} for $i \neq j$ and in particular on U/t.[13]

The ground-state energy E_{gs} and density-matrix $\gamma_{ij}^{\mathrm{gs}}$ are determined by minimizing the energy functional

$$E[\gamma] = E_K[\gamma] + W[\gamma] \qquad (2)$$

with respect to γ_{ij}. $E[\gamma]$ is defined for all density matrices that derive from a physical state, i.e., that can be written as

$$\gamma_{ij} = \sum_\sigma \gamma_{ij\sigma} = \sum_\sigma \langle \Psi | \hat{c}_{i\sigma}^\dagger \hat{c}_{j\sigma} | \Psi \rangle, \qquad (3)$$

where $|\Psi\rangle$ is an N-particle state. Such γ_{ij} are said to be pure-state N-representable. An extension of the definition domain of E to ensemble-representable density matrices Γ_{ij} is straightforward following the work by Valone.[20,21] The first term in Eq. (2) is the kinetic energy associated with the electronic motion in the lattice. It is given by

$$E_K[\gamma] = \sum_{ij} t_{ij} \gamma_{ij}, \qquad (4)$$

thus including all single-particle contributions. The second term is the interaction-energy functional given by[5]

$$W[\gamma] = \min_{\Psi \to \gamma} \left[U \sum_i \langle \Psi[\gamma] | \hat{n}_{i\uparrow} \hat{n}_{i\downarrow} | \Psi[\gamma] \rangle \right], \qquad (5)$$

where the minimization runs over all N-particle states $|\Psi[\gamma]\rangle$ that satisfy

$$\langle \Psi[\gamma] | \sum_\sigma \hat{c}_{i\sigma}^\dagger \hat{c}_{j\sigma} | \Psi[\gamma] \rangle = \gamma_{ij} \qquad (6)$$

for all i and j. $W[\gamma]$ represents the minimum value of the interaction energy compatible with a given density matrix γ_{ij}. It is a universal functional of γ_{ij} in the sense that it is independent of t_{ij}, i.e., of the system under study. However, W depends on the number of electrons N_e, on the structure of the many-body Hilbert space, as given by N_e and the number of orbitals or sites N_a, and on the form of the model interactions.[22]

$E[\gamma]$ is minimized by expressing

$$\gamma_{ij} = \sum_\sigma \gamma_{ij\sigma} = \sum_{k\sigma} u_{ik\sigma} \eta_{k\sigma} u_{jk\sigma}^* \qquad (7)$$

in terms of the eigenvalues $\eta_{k\sigma}$ (occupation numbers) and eigenvectors $u_{ik\sigma}$ (natural orbitals) of $\gamma_{ij\sigma}$. Lagrange multipliers μ and $\lambda_{k\sigma}$ ($\varepsilon_{k\sigma} = \lambda_{k\sigma}/\eta_{k\sigma}$) are introduced in order to impose the constraints $\sum_{k\sigma} \eta_{k\sigma} = N_e$ and $\sum_i |u_{ik\sigma}|^2 = 1$. Deriving with respect to $u_{jk\sigma}^*$ and $\eta_{k\sigma}$ ($0 \leq \eta_{k\sigma} \leq 1$), one obtains the eigenvalue equations[17,19]

$$\sum_i \left(t_{ij} + \frac{\partial W}{\partial \gamma_{ij\sigma}} \right) u_{ik\sigma} = \varepsilon_{k\sigma} u_{jk\sigma}, \tag{8}$$

with the subsidiary conditions $\varepsilon_{k\sigma} < \mu$ if $\eta_{k\sigma} = 1$, $\varepsilon_{k\sigma} = \mu$ if $0 < \eta_{k\sigma} < 1$, and $\varepsilon_{k\sigma} > \mu$ if $\eta_{k\sigma} = 0$. Self-consistency is implied by the dependence of $\partial W / \partial \gamma_{ij\sigma}$ on $\eta_{k\sigma}$ and $u_{ik\sigma}$. This formulation is analogous to density-matrix functional theory in the continuum.[19] However, it differs from KS-like approaches which assume noninteracting v-representability and where only integer occupations are allowed.[13,14] In the present case, the fractional occupations of natural orbitals play a central role. One may in fact show that in general $0 < \eta_{k\sigma} < 1$ for all $k\sigma$. Exceptions are found in very special situations like the uncorrelated limit ($U = 0$) or the fully polarized ferromagnetic state in the Hubbard model ($S_z = \min\{N_e, 2N_a - N_e\}/2$). This can be understood from perturbation-theory arguments —none of the $\eta_{k\sigma}$ is a good quantum number for $U \neq 0$—and is explicitly verified by exact solutions of the Hubbard Hamiltonian on finite systems or the 1D chain.[23] Therefore, all $\varepsilon_{k\sigma}$ in Eq. (8) must be degenerate and consequently the ground-state density matrix satisfies

$$t_{ij} + \frac{\partial W}{\partial \gamma_{ij\sigma}} = \delta_{ij} \mu. \tag{9}$$

Notice the importance of the dependence of W on the off-diagonal density-matrix elements γ_{ij} which measure the degree of electron localization. Approximations of W in terms of the diagonal γ_{ii} alone are not applicable in this framework ($t_{ij} \neq 0$ for NN ij). Equation (9) provides a self-consistent scheme to obtain the ground-state γ_{ij}^{gs} according to the variational principle. In Sec. III we present and discuss simple explicit approximations to $W[\gamma]$ that are intended to describe the electronic properties of the Hubbard model in different interaction regimes, band-fillings, and lattice structures.

III. INTERACTION-ENERGY FUNCTIONAL IN THE HUBBARD MODEL

The general functional $W[\gamma]$, valid for all lattice structures and for all types of hybridizations, can be simplified at the expense of universality if the hopping integrals are short ranged. For example, if only NN hoppings are considered, the kinetic energy E_K is independent of the density-matrix elements between sites that are not NNs. Therefore, the constrained search in Eq. (5) may be restricted to the $|\Psi[\gamma]\rangle$ that satisfy Eq. (6) only for $i = j$ and for NN ij. This reduces significantly the number of variables in $W[\gamma]$ and renders the determination and interpretation of the functional dependence far simpler. In particular for periodic lattices the ground-state γ_{ij}^{gs} is translational invariant. Therefore, in order to determine E_{gs} and γ_{ij}^{gs}, one may set $\gamma_{ii} = n = N_e/N_a$ for all sites i, and $\gamma_{ij} = \gamma_{12}$ for all NN pairs ij. In this case the interaction energy can be regarded as a simple function $W(\gamma_{12})$ of the density-matrix element between NNs. This is certainly a great practical advantage. However, it should be noted that restricting the minimization constraints in Eqs. (5)

and (6) to NN γ_{ij} also implies that W loses its universal character, since the NN map and the resulting dependence of W on γ_{12} are in principle different for different lattice structures.

The difficulties introduced by the lack of universality can be overcome by taking advantage of the scaling properties $W(\gamma_{12})$. Recent numerical studies[16] have in fact shown that W is nearly independent of system size N_a, band filling $n = N_e/N_a$, and lattice structure, if W is measured in units of the Hartree–Fock energy $E_{HF} = U n^2/4$ and if γ_{12} is scaled within the relevant domain of representability $[\gamma_{12}^\infty, \gamma_{12}^0]$. Here, γ_{12}^0 stands for the largest possible value of the NN bond order γ_{12} for a given N_a, n, and lattice structure. It represents the maximum degree of electron delocalization and corresponds to the uncorrelated limit. On the other side, γ_{12}^∞ refers to the strongly correlated limit of γ_{12}, i.e., to the largest NN bond order that can be obtained under the constraint of vanishing W. For half-band filling $\gamma_{12}^\infty = 0$, while for $n \neq 1$, $\gamma_{12}^\infty > 0$.[24] Physically, the possibility of scaling the interaction energy means that the relative change in W associated with a given change in the degree of electron delocalization $g_{12} = (\gamma_{12} - \gamma_{12}^\infty)/(\gamma_{12}^0 - \gamma_{12}^\infty)$ can be regarded as nearly independent of the system under study. This pseudo-universal behavior of W/E_{HF} as a function of g_{12} can be exploited to obtain good general approximations to $W(\gamma_{12})$ by applying such a scaling to the functional dependence derived from a simple reference system or from known limits.

In a previous paper we proposed an approximation to the interaction energy W of the Hubbard model by extracting the functional dependence from the exact result for the Hubbard dimer, which is given by[17]

$$W^{(2)} = E_{HF}(1 - \sqrt{1 - g_{12}^2}). \tag{10}$$

This very simple expression satisfies several general properties of the exact $W(\gamma_{12})$.

(i) For $\gamma_{12} = \gamma_{12}^0$, $W^{(2)} = E_{HF}$ since the underlying electronic state $\Psi[\gamma_{12}^0]$ is a single Slater determinant. Moreover, one observes that $\partial W^{(2)}/\partial \gamma_{12} = \infty$ for $\gamma_{12} = \gamma_{12}^0$. This is a necessary condition in order that $\gamma_{12}^{gs} < \gamma_{12}^0$ already for arbitrary small $U/t \neq 0$, as expected from perturbation theory.

(ii) $W^{(2)}(\gamma_{12})$ decreases monotonously with decreasing γ_{12} reaching its lowest possible value, $W = 0$, for $\gamma_{12} = \gamma_{12}^\infty$. In other words, a reduction of the interaction energy is obtained at the expense of electron delocalization.

(iii) In the strongly correlated limit ($\gamma_{12} \ll \gamma_{12}^0$) one observes that $W^{(2)} \propto \gamma_{12}^2$. Therefore, for $U/t \gg 1$, $\gamma^{gs} \propto t/U$ and $E_{gs} \propto t^2/U$, a well-known result in the Heisenberg limit of the half-filled Hubbard model.[9]

A correct description of these basic properties and of the dependence of W/E_{HF} on g_{12} are at the origin of the remarkable performance of this simple dimer ansatz in the description of several ground-state properties of the Hubbard model.[17]

In order to discuss the strongly correlated limit of Eq. (10) in more detail we expand $W^{(2)}$ to lowest order in γ_{12}. At half-band filling one obtains

$$W^{(2)} = (1/8)\alpha_2 U \gamma_{12}^2 + \mathcal{O}(\gamma_{12}^4) \qquad (11)$$

with $\alpha_2 = (\gamma_{12}^0)^{-2}$. The exact interaction-energy W_{ex} is also proportional to $U\gamma_{12}^2$ in the limit of small γ_{12}. Therefore, W_{ex} can be expanded in the same form as Eq. (11) but with a somewhat different coefficient α_{ex}. Notice that in the case of the Hubbard dimer, we have $\gamma_{12}^0 = 1$ and $\alpha_2^{dim} = 1$, which coincides of course with the exact result. Considering for example the 1D chain, the 2D square lattice, and the three-dimensional (3D) simple-cubic lattice one finds that the leading coefficients resulting from Eq. (10) are $\alpha_2^{1D} = (\pi/2)^2 \simeq 2.47$, $\alpha_2^{2D} = 6.09$, and $\alpha_2^{3D} = 9.30$. These can be compared with the corresponding exact result derived from the Bethe-ansatz solution of the 1D Hubbard chain,[23] or with perturbation-theory calculations for the square and simple-cubic lattices,[25] which are given by $\alpha_{ex}^{1D} = 2/\ln 2 \simeq 2.89$, $\alpha_{ex}^{2D} = 6.91$, and $\alpha_{ex}^{3D} = 10.94$. One observes that Eq. (10) reproduces correctly the trends in α with increasing dimensions. However, there is also a systematic underestimation of the interaction energy of the order of 12%–15%. These quantitative discrepancies have direct consequences on the predicted properties, since the behavior of W for small γ_{12} determines the ground-state density matrix γ_{12}^{gs} and energy E_{gs} in the strongly correlated limit. In fact, approximating W as in Eq. (11), writing the kinetic energy as $E_K = zt\gamma_{12}$, where z is the coordination number, and using Eq. (9), one obtains $\gamma_{12}^{gs} = (4z/\alpha)(t/U)$ and $E_{gs} = -(2z^2/\alpha)(t^2/U)$. Thus, an inaccuracy in α results in a similar relative error in γ_{12}^{gs} and E_{gs} for $U/t \gg 1$.

To overcome these shortcomings more flexible approximations to the interaction-energy functional are needed, which allow one to go beyond Eq. (10). Therefore, we propose a general ansatz of the form

$$W^{(n)} = E_{HF}[1 - \sqrt{P_n(g_{12})}], \qquad (12)$$

where $P_n(g_{12})$ is a function of $g_{12} = (\gamma_{12} - \gamma_{12}^\infty)/(\gamma_{12}^0 - \gamma_{12}^\infty)$, thus incorporating the scaling properties of W without loss of generality. $P_n(g_{12})$ is approximated by an n-order polynomial $P_n(g_{12}) = \Sigma_{k=0}^n a_k g_{12}^k$. This is justified by the fact that $(W - E_{HF})^2$ is in general a well-behaved function of g_{12}, even in the uncorrelated limit where $\partial W/\partial \gamma_{12}$ diverges ($g_{12} = 1$). The coefficients a_k are to be determined from known properties of W. First of all, one observes that at half-band filling, and for bipartite lattices in general, the sign of γ_{12} can be changed without altering W. Thus, $P_n(g_{12})$ is an even function of g_{12} and $a_k = 0$ for odd k ($\gamma_{12}^{0-} = -\gamma_{12}^{0+}$ and $\gamma_{12}^{\infty-} = -\gamma_{12}^{\infty+}$). In nonbipartite lattices away from half-band filling one may also set for simplicity $a_k = 0$ for odd k, since the dependence on g_{12} is very similar for positive and negative γ_{12}, once the different domains of representability are scaled.[16,24]

The uncorrelated and fully correlated limits of W ($W = E_{HF}$ for $g_{12} = 1$, and $W = 0$ for $g_{12} = 0$) impose two simple conditions on the a_k, namely, $P_n(1) = \Sigma_k a_k = 0$ and $P_n(0) = a_0 = 1$. This defines the second-order approximation $W^{(2)}$ completely. In this case, $P_2(g_{12}) = 1 - g_{12}^2$, which coincides with the above-discussed dimer ansatz [Eq. (10)]. The two approaches are therefore consistent. The dimer ansatz can be regarded as the simplest polynomial-based approximation of W, as given by Eq. (12), that satisfies the obvious limits.

The fourth-order approximation $W^{(4)}$ introduces the aimed additional flexibility that can be exploited to reproduce the strongly correlated limit of W exactly. Expanding Eq. (12) to second order in γ_{12} one observes that at half-band filling this is achieved when $a_0 = 1$, $a_2 = -\alpha_{ex}(\gamma_{12}^0)^2 = -\alpha_{ex}/\alpha_2$, and $a_4 = -(a_0 + a_2)$. Thus, the fourth-order approximation to W is given by

$$W^{(4)} = E_{HF}(1 - \sqrt{1 - \kappa g_{12}^2 + (\kappa - 1)g_{12}^4}), \qquad (13)$$

where $\kappa = \alpha_{ex}/\alpha_2 > 0$ is the ratio between the small-γ_{12} expansion coefficients of W^{ex} and $W^{(2)}$. The value of κ depends on the lattice structure or system dimensions. At half-band filling it can be determined by applying perturbation theory to the Heisenberg limit of the Hubbard model.[25] For instance, for the 1D chain, 2D square lattice, and 3D simple-cubic lattice one obtains, respectively, $\kappa_{1D} = 8/(\pi^2 \ln 2) = 1.169$, $\kappa_{2D} = 1.135$, and $\kappa_{3D} = 1.176$. Notice that κ depends rather weakly on the lattice structure and that it is not very far from the dimer value $\kappa = 1$, for which Eq. (13) reduces to Eq. (10). Therefore, the fourth-order term appears as a relatively small correction to the second-order approximation. Higher-order polynomial approximations to W could be derived in an analogous way, provided that reliable information is available on the following terms of the small-γ_{ij} expansion of W^{ex}. This gives the possibility of further improving the accuracy of the results by incorporating a more detailed description of the strongly correlated limit.

In Fig. 1 the approximate interaction energies $W^{(2)}$ and $W^{(4)}$ of the half-filled 1D Hubbard chain are compared with the corresponding exact result W^{ex}, as derived from the Bethe-ansatz solution.[23] As already observed,[17] even the simplest dimer ansatz $W^{(2)}$ follows $W^{ex}(\gamma_{12})$ quite closely all along the crossover from weak to strong correlations. In this case the interaction energy is always underestimated, and the absolute value of the relative error $\epsilon = |W - W^{ex}|/W^{ex}$ increases monotonously as γ_{12} decreases, reaching about 15% for $\gamma_{12}/\gamma_{12}^0 < 0.4$. The fourth-order approximation provides a significant advance, not only for $\gamma_{12}/\gamma_{12}^0 \ll 1$ but in the complete domain of representability. For $W^{(4)}$ the relative error ϵ is reduced to less than 1% for $\gamma_{12}/\gamma_{12}^0 < 0.4$ ($\epsilon \to 0$ for $\gamma_{12} \to 0$). The largest discrepancies are found for $\gamma_{12}/\gamma_{12}^0 \simeq 0.8$–0.9, where ϵ reaches only 3%. An appreciable improvement in the accuracy of the derived properties can be therefore expected. In the following sections, Eqs. (10) and (13) are applied in the framework of LDFT to determine several electronic properties of the Hubbard model in 1D, 2D, and 3D periodic lattices.

IV. GROUND STATE ENERGY

In Fig. 2 the ground-state energy E_{gs} of the half-filled 1D Hubbard model is given as a function of the Coulomb repulsion strength U/t. Comparison between LDFT and the Bethe-ansatz exact solution shows that the fourth-order approximation improves significantly the already good results
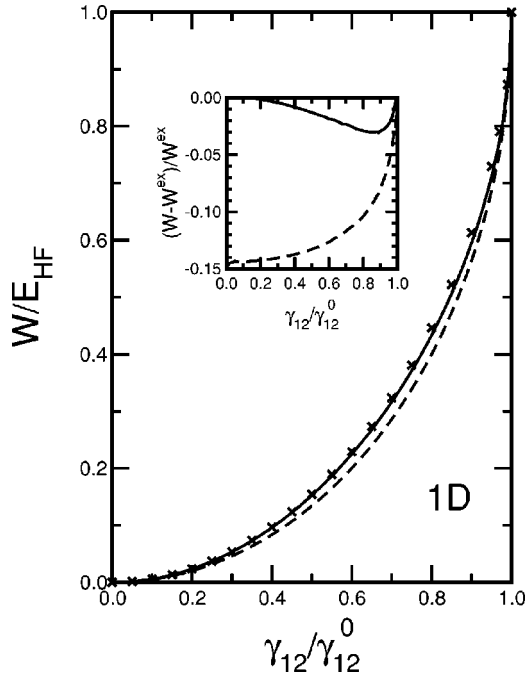
FIG. 1. Interaction energy $W(\gamma_{12})$ of the one-dimensional (1D) Hubbard model at half-band filling ($n=1$) as a function of the density-matrix element or bond order γ_{12} between nearest neighbors. γ_{12}^0 refers to the ground-state bond order in the uncorrelated limit ($U=0$). Results are given for the dimer approximation $W^{(2)}$ [Eq. (10), dashed], the fourth-order approximation $W^{(4)}$ [Eq. (13) with $\kappa=\kappa_{1D}\simeq1.169$, solid], and the exact W^{ex} [Eq. (5), crosses] which is derived from the Bethe ansatz solution (Ref. 23). In the inset the corresponding relative errors are shown.
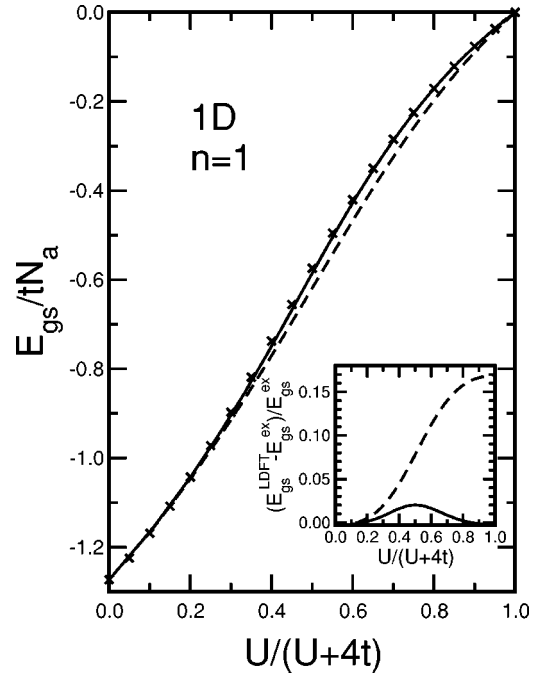
FIG. 2. Ground-state energy E_{gs} of the half-filled 1D Hubbard model as a function of the Coulomb repulsion strength U/t. The dashed curves refer to lattice density-functional theory (LDFT) using the dimer approximation to W [Eq. (10)] and the solid curves to the fourth-order approximation [Eq. (13) with $\kappa=\kappa_{1D}=1.169$]. The crosses are the exact results derived from the Bethe-ansatz solution (Ref. 23). The corresponding relative errors are given in the inset.

derived using the dimer ansatz.[17] This concerns not only the strongly correlated limit where, as expected, $W^{(4)}$ recovers the exact result, but the complete range of U/t. The largest quantitative discrepancies between exact and fourth-order results are in fact very small. They amount to less than 3% and are found for intermediate interaction strengths ($U/t\simeq4$). In contrast, the relative error in the dimer ansatz increases monotonously with U/t reaching about 17% for $U/t=\infty$ (see the inset of Fig. 2). It is interesting to note that in both cases no artificial symmetry breaking is required in order to describe correctly the electron localization induced by correlations and the resulting dependence of E_{gs} on U/t, as is often the case in other mean-field approaches.

The higher performance obtained with the fourth-order correction originates in an improved accuracy of both kinetic and Coulomb contributions to the ground-state energy. As shown in Fig. 3, the kinetic energy $E_K<0$ increases monotonously with increasing U/t, first rather slowly up to $U/t\simeq4$, and then more rapidly when electron localization starts to set in. For $U/t\lesssim4$, the values of E_K obtained using $W^{(2)}$ and $W^{(4)}$ are very close to the exact result (typically $|E_K^{(2)}-E_K^{ex}|/E_K^{ex}\lesssim2.6\%$ and $|E_K^{(4)}-E_K^{ex}|/E_K^{ex}\lesssim2.0\%$). For $U/t>4$ the dimer ansatz shows some limitations while the fourth-order approximation remains very accurate (for example, for $U/t=12$, $|E_K^{(2)}-E_K^{ex}|/E_K^{ex}\simeq13\%$ and $|E_K^{(4)}-E_K^{ex}|/E_K^{ex} \lesssim2.4\%$). The Coulomb energy E_C shows the usual nonmo-

notonous behavior, first increasing with U/t in the weakly correlated regime and then decreasing as the strongly correlated limit is approached. These trends are well reproduced by both second- and fourth-order approximations. However, one finds that it is in general more difficult to accurately describe E_C as compared to E_K. The second-order $E_C^{(2)}$ underestimates (overestimates) E_C^{ex} appreciably for $2<U/t<5$ ($U/t>5$). The fourth-order correction provides a clear improvement over the dimer ansatz, by increasing E_C in one case ($U/t\lesssim5$) and reducing it in the other ($U/t\gtrsim10$). As for E_{gs}, the remaining differences with the exact results are quite small and correspond to intermediate U/t. Summarizing, one may observe that the accuracy of the calculated E_{gs} is not the result of a strong compensation of errors, since a very good performance is achieved for the kinetic and Coulomb energies separately.

In Fig. 4 results are given for E_{gs} of the 2D square lattice and 3D simple cubic lattice at half-band filling. For $U/t\lesssim3$ the second-order and fourth-order results are almost indistinguishable, while for $U/t>4$ the fourth-order approximation yields somewhat higher values ($E_{gs}^{(2)}<E_{gs}^{(4)}<0$). These trends are very similar to those observed in the 1D chain. The LDFT calculations for 2D and 3D systems compare well with far more demanding quantum Monte Carlo (QMC) studies[26,27] (see Fig. 4). Furthermore, the reliability of the LDFT results is confirmed by comparison with exact Lanczos diagonalizations on small clusters, for example, on a $N_a=3\times4$ cluster of the square lattice with periodic bound-
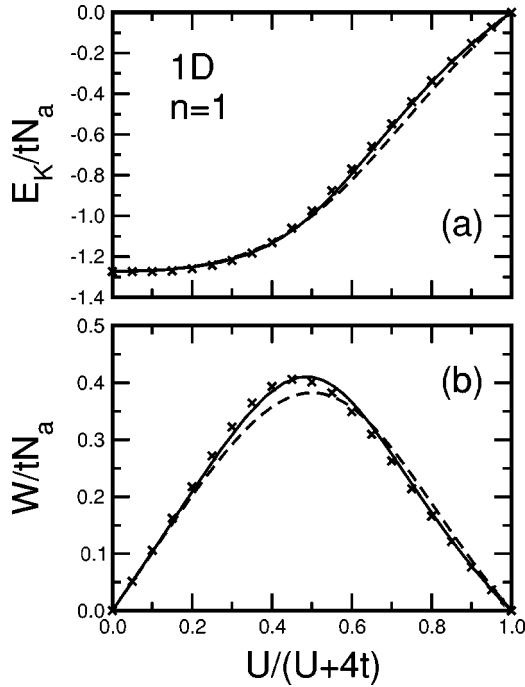
FIG. 3. (a) Kinetic energy E_K and (b) Coulomb energy E_C of the half-filled 1D Hubbard model as a function of U/t. The dashed curves correspond to the dimer approximation [Eq. (10)], the solid curves to the fourth-order approximation [Eq. (13) with $\kappa = \kappa_{1D} = 1.169$], and the crosses to the Bethe-ansatz exact solution (Ref. 23).

FIG. 4. Ground-state energy E_{gs} of the half-filled Hubbard model as a function of the Coulomb repulsion U/t: (a) two-dimensional (2D) square lattice and (b) three-dimensional (3D) simple cubic lattice. The dashed curves correspond to the dimer approximation [Eq. (10)] and the solid curves to the fourth-order approximation [Eq. (13) with (a) $\kappa = \kappa_{2D} = 1.135$ and (b) $\kappa = \kappa_{3D} = 1.176$]. The crosses with error bars refer to quantum Monte Carlo (QMC) calculations (Refs. 26 and 27).

ary conditions. In this case, like in 1D, the overall performance is very good, with the largest quantitative discrepancies being observed for intermediate values of U/t. For instance, for $U/t = 4$ one obtains $|E_{gs}^{(4)} - E_{gs}^{ex}|/|E_{gs}^{ex}| = 4.2 \times 10^{-2}$, and for $U/t = 16$ $|E_{gs}^{(4)} - E_{gs}^{ex}|/|E_{gs}^{ex}| = 3.2 \times 10^{-2}$. In conclusion, LDFT using Eq. (13) for the interaction energy W yields an accurate description of the ground-state energy of the Hubbard model in different dimensions.[28]

V. CHARGE EXCITATION GAP

The charge excitation or band gap

$$\Delta E_c = E_{gs}(N_e + 1) + E_{gs}(N_e - 1) - 2E_{gs}(N_e) \qquad (14)$$

is a property of considerable interest, which measures the low-energy excitations associated with changes in the number of electrons N_e, and which is very sensitive to the degree of electronic correlations. It can be related to the discontinuity in the derivative of the ground-state kinetic energy E_K and correlation energy $E_{corr} = E_C - E_{HF}$ with respect to band-filling n. For $N_a \rightarrow \infty$ and $n = 1$, it is given by

$$\Delta E_c = (\partial \varepsilon / \partial n)|_{1^+} - (\partial \varepsilon / \partial n)|_{1^-}, \qquad (15)$$

where $\varepsilon = (E_K + E_{corr})/N_a$. The determination of ΔE_c is in general a more difficult task than the calculation of ground-state properties like E_{gs}, E_K, and E_C. In fact, the band gap in semiconductors has been an important problem which motivated numerous works in the context of DFT in the con-
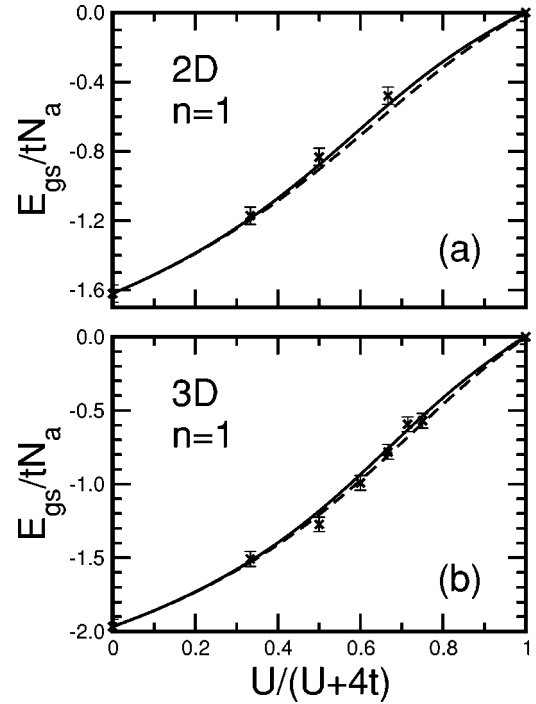
tinuum. Therefore, ΔE_c appears as a particularly interesting property to investigate with the present lattice density-functional formalism.

In the half-filled Hubbard model on bipartite lattices, ΔE_c increases with increasing U/t ($\Delta E_c = 0$ for $U/t = 0$) and approaches the limit $\Delta E_c \rightarrow (U - w_b)$ for $U/t \rightarrow \infty$, where w_b is the width of the single-particle band ($w_b = 4t$, $8t$, and $12t$ for the 1D, 2D square, and 3D simple-cubic lattices, respectively). Figure 5 presents LDFT results for ΔE_c in 1D, 2D, and 3D Hubbard models ($n = 1$). Comparison with the exact Bethe-ansatz solution for the 1D chain[23] and with available QMC calculations for the square[26] and simple cubic[27] lattices shows a good overall agreement. However, it should be noted that in the 1D case the gap is significantly overestimated for $U/t \ll 1$. Here we obtain $\Delta E_c \propto (U/t)^2$, while in the exact solution ΔE_c increases much more slowly, namely, exponentially in $-t/U$. This discrepancy concerns both the second-order and the fourth-order approximations, which are nearly indistinguishable for $U/t < 2–4$. Consequently, it is possible that the results for 2D and 3D lattices shown in Fig. 5 also overestimate the gap for small U/t. In any case, the accuracy of LDFT improves rapidly with increasing U/t, as electron localization starts to set in, and the error in ΔE_c tends to zero for large U/t. Therefore, the development of a Mott insulator in the strongly correlated limit is correctly described.

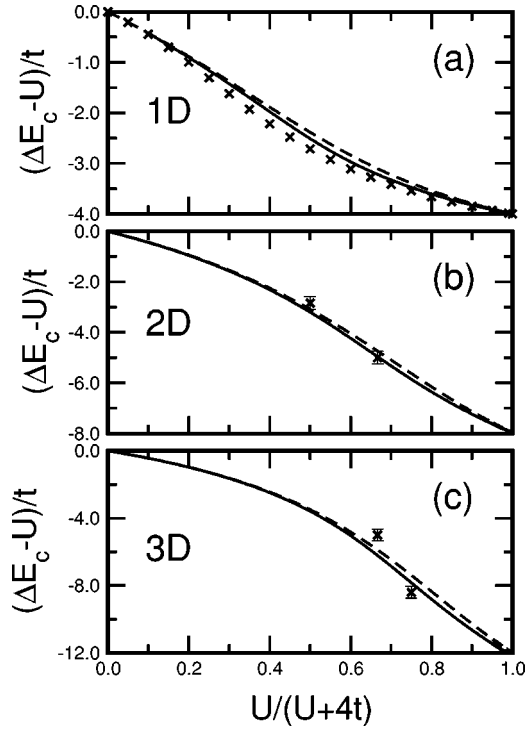It is important to remark, in the context of metal-insulator

FIG. 5. Charge excitation gap ΔE_c of the Hubbard model at half-band filling as a function of U/t: (a) 1D chain, (b) 2D square lattice, and (c) 3D simple cubic lattice. The dashed curves correspond to the dimer approximation [Eq. (10)] and the solid curves to the fourth-order approximation [Eq. (13)] with (a) $\kappa = \kappa_{1D} = 1.169$, (b) $\kappa = \kappa_{2D} = 1.135$, and (c) $\kappa = \kappa_{3D} = 1.176$. The crosses refer to exact results in the 1D chain (Ref. 23) and to QMC calculations in 2D (Ref. 26) and 3D lattices (Ref. 27).

transitions in three dimensions, that our calculations on the SC lattice yield a finite gap $\Delta E_c > 0$ for $n = 1$ and all $U/t > 0$. This is consistent with previous results on 3D bipartite lattices, which are expected to be antiferromagnetic (AF) insulators for all $U/t > 0$.[11,12] The functionals $W^{(2)}$ and $W^{(4)}$ correctly reproduce this behavior, as well as the formation of local moments $\langle S_i^2 \rangle = 3(1 - 2\langle \hat{n}_{i\uparrow}\hat{n}_{i\downarrow}\rangle)/4$, without involving a spin-density-wave symmetry breaking. This can be understood by recalling that they are based on the exact functional of the Hubbard dimer which, being a bipartite cluster, incorporates AF correlations ($n = 1$). However, the properties change qualitatively if frustrations become important (e.g., in nonbipartite lattices or if second NN hoppings are significantly large). In this case it has been shown that the half-filled Hubbard model is a metal with $\Delta E_c = 0$ for small $U > 0$ and that a metal-insulator transition takes place at a finite interaction strength U_c, which is of the order of the single-particle band width w_b.[11] This behavior is not reproduced by the functionals $W^{(2)}$ and $W^{(4)}$, even if they are applied to compact lattices (e.g., the face-centered cubic lattice), since they are free from any singularities throughout the domain of representability (except for $g_{12} = 1$) and since the resulting γ_{ij}^{gs} are smooth functions of U/t. Notice that the exact functional W_{ex} may show a far more complex behavior, particularly if the nature of the state $|\Psi[\gamma]\rangle$ yielding the minimum of Eq. (5) changes as a function of γ. This is expected to be

the case at a metal-insulator transition, where a discontinuous decrease of $\langle \hat{n}_{i\uparrow}\hat{n}_{i\downarrow}\rangle$ occurs. Finally, let us point out that the results derived from Eqs. (10) and (13) for large U/t ($U > U_c$) are consistent with previous studies. This concerns not only the presence of a finite gap ΔE_c, but also the fact that the number of double occupations does not vanish on the insulating side of the transition.[11,12]

Comparing second- and fourth-order approximations for $U/t > 2$–4 one observes that the charge gap is always somewhat smaller in the latter case. For the 1D chain, the reduction of ΔE_c due to the fourth-order correction improves the agreement with the exact solution appreciably (e.g., $|\Delta E_c^{(4)} - \Delta E_c^{ex}| \simeq |\Delta E_c^{(2)} - \Delta E_c^{ex}|/2$ for $U/t > 10$). In the considered 2D and 3D lattices, the differences between second- and fourth-order results are similar to those observed in the 1D chain. Comparison with QMC calculations shows a good overall agreement although some quantitative differences can be noted. For example, as shown in Fig. 5, our values for ΔE_c are somewhat smaller than the QMC ones for the 2D (3D) lattice with $U/t = 4$ ($U/t = 8$) and somewhat larger for $U/t = 8$ ($U/t = 12$). In summary, the ensemble of 1D, 2D, and 3D results shows that LDFT provides a very simple and efficient method of calculating the charge excitation energies of the Hubbard model in different dimensions and interaction regimes. However, the proposed approximations to W are still not quite satisfactory in the weakly correlated limit and deserve to be improved.

VI. CHARGE SUSCEPTIBILITY

The charge susceptibility χ_c is defined by

$$\chi_c = \frac{dn}{d\mu}, \qquad (16)$$

where $n = N_e/N_a$ is the number of electrons per site and μ the chemical potential. It represents the many-body density of electronic states at the Fermi energy μ and thus provides very useful information on the low-energy charge-excitation spectrum as a function of band filling. In Figs. 6–8 χ_c is given as a function of μ for 1D, 2D, and 3D Hubbard models on bipartite lattices for representative values of U/t. The LDFT calculations reported in these figures were performed using the dimer ansatz for W given by Eq. (10). As will be discussed in the following, the fourth-order approximation [Eq. (13)] yields very similar results. In the case of the 1D chain comparison is made with the exact $\chi_c(\mu)$, which is obtained from the Bethe ansatz solution.[23] For the 2D square lattice, we also show ground-state QMC results[26] for $U/t = 4$. Notice that in bipartite lattices, as those considered here, electron–hole symmetry implies that χ_c is the same for band fillings n and $n' = 2 - n$, and therefore $\chi_c(\mu) = \chi_c(\mu' = U - \mu)$.

In the absence of interactions χ_c coincides with the single-particle density of states of the corresponding lattices ($U = 0$). These are gapless and show the usual van Hove singularities at the band edges $\mu = \pm w_b/2$ and at some points within the bands of the square and simple-cubic lattices. For finite U a gap $\Delta E_c = \mu(n = 1^+) - \mu(n = 1^-)$ opens at half-
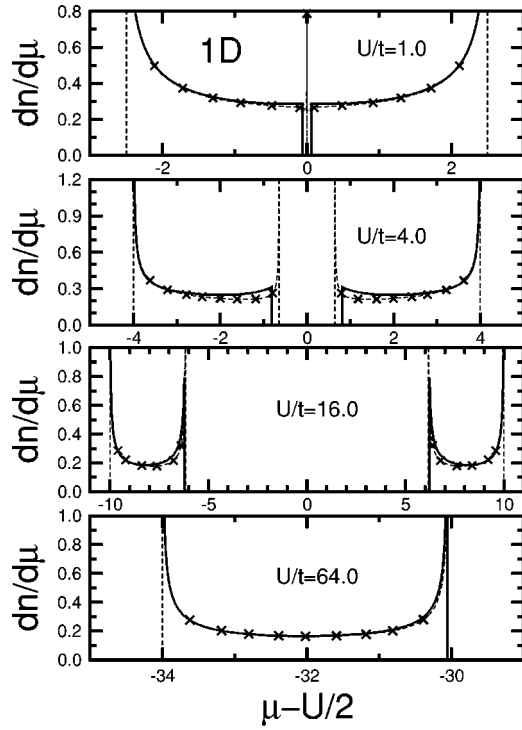
FIG. 6. Charge susceptibility χ_c of the 1D Hubbard model as a function of the chemical potential μ for different Coulomb repulsions U/t. The solid curves refer to LDFT in the dimer approximation [Eq. (10)] and the dashed curves with crosses to the exact Bethe ansatz solution (Ref. 23). For $U/t=64$ only the lower Hubbard band is shown.

FIG. 7. Charge susceptibility χ_c of the Hubbard model on a 2D square lattice as a function of the chemical potential μ for different Coulomb repulsions U/t. The solid curves are obtained using LDFT and the dimer approximation to the interaction-energy functional [Eq. (10)]. The crosses for $U/t=4$ refer to ground-state QMC calculations (Ref. 26). For $U/t=64$ only the lower Hubbard band is shown.

band filling which increases monotonously with U, as discussed in Sec. V. Thus, the two so-called lower and upper Hubbard bands start to be distinguished, which correspond to hole and electron doping, respectively. The separation of the bands becomes particularly clear for $U \approx w_b$, when ΔE_c reaches values of the order of single-particle band width w_b (see Figs. 6–8). At the same time the width of the lower and upper bands increases with U, from $w_b/2$ for $U=0^+$, to w_b for $U=+\infty$. These qualitative features are common to bipartite lattices in all dimensions and are correctly described by LDFT.

In the 1D case, where a detailed comparison with the exact solution is possible, we observe that our results are very accurate except close to half-band filling and for small or moderate values of U/t (see Fig. 6). The nature of the discrepancies close to $n=1$ is basically twofold. First, we find again the overestimation of the band gap ΔE_c, which is relatively important for small U/t (see also Sec. V). Consequently, the band edges $\mu(n=1^-)$ and $\mu(n=1^+)$ are not precisely reproduced in this limit, even if the absolute error $\epsilon = |\mu - \mu^{ex}|$ always remains reasonably small. The largest inaccuracies are found for $U/t \simeq 3$ and amount to $\epsilon/w_b = 8.1 \times 10^{-2}$. Nevertheless, this problem disappears as U/t increases, since ϵ tends rapidly to zero in the strongly correlated limit (e.g., $\epsilon/w_b = 1.2 \times 10^{-4}$ for $U/t=16$). The second limitation concerns the shape of χ_c close to half-band filling. The exact solution of the 1D chain shows sharp divergences in χ_c at the gap edges $\mu(n=1^-)$ and $\mu(n=1^+)$ for $U>0$,
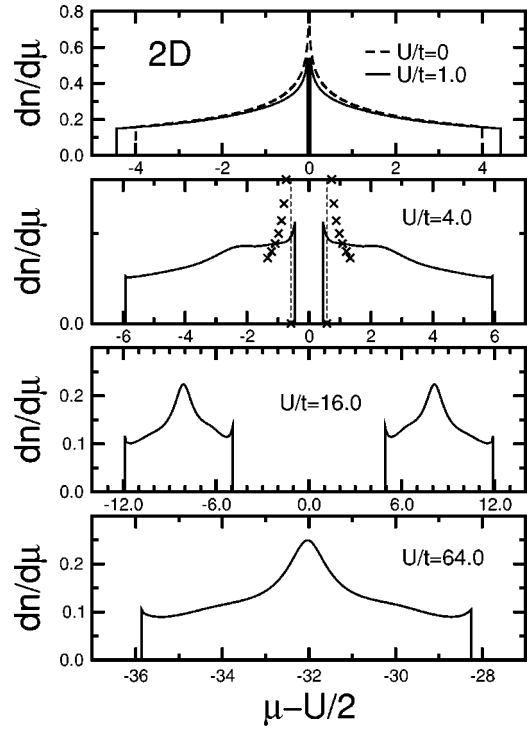
which we fail to reproduce. For small and moderate U/t, for example $U/t=1$ or 4, we obtain a nearly constant χ_c for $\mu \to \mu(n=1^{\pm})$, while the exact result is $\chi_c \to +\infty$ (see Fig. 6). Notice, however, that the increase and divergence of χ_c^{ex} are sharply localized in a narrow range of μ, particularly for small U/t. The divergence of χ_c for $n \to 1$ could be reproduced by considering broken symmetry solutions of the LDFT equations, like in the AF Hartree–Fock approximation. Even so, it would be more interesting to describe this effect without involving a symmetry breaking, which is known to be artificial, and which could affect the results on the kinetic, Coulomb, and total energies, particularly in the case of finite systems.[29] As we approach the strongly correlated limit the LDFT results for χ_c develop peaks at the gap edges, which height increases with U/t, thus approaching asymptotically the exact result. Still, χ_c always remains finite for all finite U/t (see Fig. 6 for $U/t=16$ and 64). The very good performance for large U/t can be understood by recalling that for $U/t=+\infty$, the LDFT results correspond to the fully polarized or Nagaoka state,[30] which is the exact ground state in 1D for all n ($U/t=+\infty$).[23] In higher dimensions it is possible that our calculations yield a finite-height peak for $n \to 1$, where a true divergence of χ_c could be present. This seems to be the case in the 2D square lattice where we observe narrow peaks in χ_c at the band edges. In fact ground-state QMC calculations on the square lattice with $U/t=4$ predict a divergent χ_c at half-band filling (see
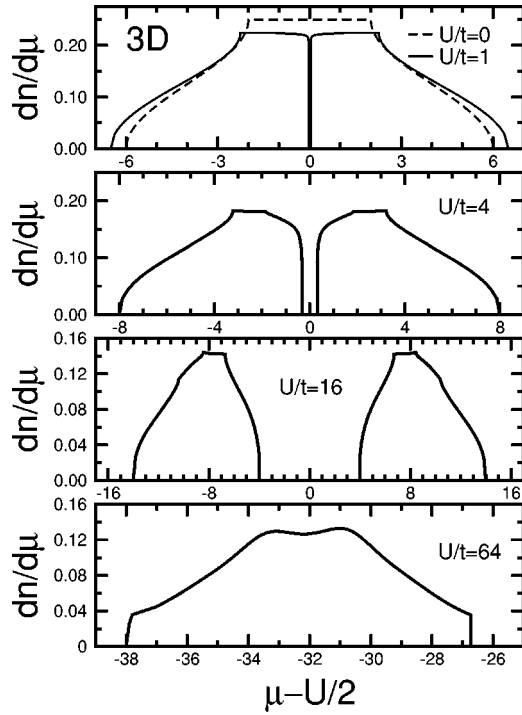
FIG. 8. Charge susceptibility χ_c of the Hubbard model on a 3D simple cubic lattice as a function of the chemical potential μ for different Coulomb repulsions U/t. The results are obtained using the dimer approximation to the interaction-energy functional [Eq. (10)]. For $U/t=64$ only the lower Hubbard band is shown.

Fig. 7). In contrast, no such peaks are found in our calculations of χ_c for the 3D simple-cubic lattice (see Fig. 8).

As already discussed in Sec. V, it is important to remark that the results presented in Fig. 8 are representative of bipartite lattices which at the half-band filling show an AF insulating behavior for all $U/t>0$. In this case of our results are in good qualitative agreement with previous studies. The obtained simple Hubbard-approximation-like structure of χ_c, with a lower and upper Hubbard bands, also applies to frustrated lattices or to paramagnetic phases provided that U/t is sufficiently large to bring the system on the insulating side of the metal-insulator transition ($U>U_c$).[11,12] However, it has been shown that the presence of frustrations drives the system into an AF *metallic* state at small U/t which contrasts with the AF insulator found in the absence of frustrations.[11] In this case the spectral density presents—in addition to a progressive development of lower and upper Hubbard bands with increasing U/t—a Kondo-like resonance at half-band filling ($\mu-U/2=0$). This resonance is characterized by a constant-height peak having a width that decreases with increasing U/t and that vanishes at U_c, i.e., at the transition to the insulating state (see Ref. 11). The functionals $W^{(2)}$ or $W^{(4)}$ fail to reproduce this kind of behavior, even when applied to compact structures (e.g., fcc lattice). This limitation does not seem surprising, since Eqs. (10) and (13) were derived from the properties of a bipartite system, and since the extensions presented in this paper, while achieving an accurate W in the strongly correlated limit at half-band filling, do not aim a very precise description at small U/t and as a

function of n. Exploring the functional dependence of W in frustrated structures, particularly close to $n=1$ and $g_{12}\simeq1$, should provide very useful clues in view of developing practical approximations to W capable of describing these remarkable effects in the framework of LDFT.

Let us finally point out that we have also determined χ_c using $W^{(4)}$ as approximate interaction energy [Eq. (13)] and found that the results are very similar to those obtained using $W^{(2)}$ and shown in Figs. 6–8. In both cases the results are extremely good away from half-band filling, nearly indistinguishable from the 1D exact solution. Close to $n=1$, the fourth-order calculations yield smaller ΔE_c and thus perform slightly better for $U/t\lesssim4$. However, the divergences of χ_c at the gap edges are not reproduced. Therefore, the fourth-order corrections do not provide a significant improvement over the dimer ansatz concerning χ_c of the 1D chain. This is probably related to the simple form considered for $W^{(4)}$ which uses a coefficient κ that is independent of n [see Eq. (13)]. While this approximation seems satisfactory for applications that concern a fixed band filling, it appears as a limitation for properties like ΔE_c or χ_c, where a precise description of the dependence of W on n is crucial. For 2D and 3D lattices the fourth-order results for χ_c are also very similar to those shown in Figs. 7 and 8.

VII. DISCUSSION

A new approximation to the interaction-energy functional $W[\gamma]$ of the Hubbard model has been proposed in the framework of lattice density functional theory, which exactly recovers the limit of strong electron correlations at half-band filling. The simpler ansatz which was derived from the functional dependence of W in the Hubbard dimer[17] is thereby extended and improved. A more accurate description of W is achieved throughout the domain of representability of γ_{ij} including the crossover from weak to strong correlations. Several properties have been determined by applying this functional to one-, two-, and three-dimensional lattices. Ground state energies, as well as kinetic and Coulomb energies, were successfully determined in all dimensions and interaction regimes. Very good results are also obtained concerning the charge-excitation gap ΔE_c and the charge susceptibility χ_c of bipartite lattices, except very close to half-band filling ($n=1$) and for small values of the Coulomb repulsion strength ($U/t\lesssim4$). This reveals some limitations in the description of the band-filling dependence of W for $n\simeq1$ and $\gamma_{12}\simeq\gamma_{12}^0$, which deserve more detailed investigations. Further insight into the origin of this problem could be obtained, for example, by analyzing the properties of the exact W as derived from the Bethe ansatz exact solution of the 1D chain and from Lanczos diagonalizations in finite 2D clusters with periodic boundary conditions. Moreover, the functional dependence of W could be determined in the limit of large γ_{12} (i.e., $\gamma_{12}\rightarrow\gamma_{12}^0$ corresponding to the weak correlations) by applying perturbation theory for small U/t. In this way, more accurate approximations to W could be developed in order to improve the results on ΔE_c and χ_c in this limit, particularly concerning the differences between bipartite and nonbipartite lattices.

Besides these methodological aspects, the accuracy of the

results and the simplicity of the calculations encourage new applications of the present approach to related problems of current interest like, for example, dimerized one-dimensional chains and ladders, the 2D square lattice with competing first and second nearest-neighbor hoppings, the properties of π electrons in doped fullerenes and nanotubes in the framework of Hubbard or PPP models, or the connection with the continuum's DFT using minimal basis sets. In this way, a novel density-functional route to the physics of strongly correlated fermions is opened.

[1] P. Hohenberg and W. Kohn, Phys. Rev. **136**, B864 (1964).

[2] W. Kohn and L.J. Sham, Phys. Rev. **140**, A1133 (1965).

[3] R.G. Parr and W. Yang, *Density-Functional Theory of Atoms and Molecules* (Clarendon, Oxford, 1989).

[4] R.M. Dreizler and E.K.U. Gross, *Density Functional Theory* (Springer, Berlin, 1990), and references therein.

[5] M. Levy, Proc. Natl. Acad. Sci. U.S.A. **76**, 6062 (1979).

[6] P.W. Anderson, Phys. Rev. **124**, 41 (1961).

[7] J. Hubbard, Proc. R. Soc. London, Ser. A **276**, 238 (1963); **281**, 401 (1964); J. Kanamori, Prog. Theor. Phys. **30**, 275 (1963); M.C. Gutzwiller, Phys. Rev. Lett. **10**, 159 (1963).

[8] R. Pariser and R.G. Parr, J. Chem. Phys. **21**, 466 (1953); **21**, 767 (1953); J. A. Pople, Trans. Faraday Soc. **49**, 1375 (1953).

[9] See, for instance, P. Fulde, *Electron Correlations in Molecules and Solids* (Springer, Berlin, 1991); N.H. March, *Electron Correlation in Molecules and Condensed Phases* (Plenum, New York, 1996).

[10] E. Dagotto, Rev. Mod. Phys. **66**, 763 (1994).

[11] A. Georges, G. Kotliar, W. Krauth, and M.J. Rozenberg, Rev. Mod. Phys. **68**, 13 (1996).

[12] M. Imada, A. Fujimori, and Y. Tokura, Rev. Mod. Phys. **70**, 1039 (1998).

[13] O. Gunnarsson and K. Schönhammer, Phys. Rev. Lett. **56**, 1968 (1986); A. Svane and O. Gunnarsson, Phys. Rev. B **37**, 9919 (1988); K. Schönhammer, O. Gunnarsson, and R.M. Noack, *ibid.* **52**, 2504 (1995).

[14] A. Schindlmayr and R.W. Godby, Phys. Rev. B **51**, 10 427 (1995).

[15] A.E. Carlsson, Phys. Rev. B **56**, 12 058 (1997); R.G. Hennig and A.E. Carlsson, *ibid.* **63**, 115116 (2001).

[16] R. López-Sandoval and G.M. Pastor, Phys. Rev. B **61**, 1764 (2000).

[17] R. López-Sandoval and G.M. Pastor, Phys. Rev. B **66**, 155118 (2002).

[18] R. López-Sandoval and G.M. Pastor, Phys. Rev. B **67**, 035115 (2003).

[19] T.L. Gilbert, Phys. Rev. B **12**, 2111 (1975). For more recent studies see, for example, S. Goedecker and C.J. Umrigar, Phys. Rev. Lett. **81**, 866 (1998), and references therein.

[20] S.M. Valone, J. Chem. Phys. **73**, 1344 (1980); **73**, 4653 (1980).

[21] Ensemble density-matrices are written as $\Gamma_{ij} = \Sigma_n w_n \langle \Psi_n | \Sigma_\sigma \hat{c}_{i\sigma}^\dagger \hat{c}_{j\sigma} | \Psi_n \rangle$ with $w_n \geq 0$ and $\Sigma_n w_n = 1$. In practice, they are much easier to characterize than pure-state density matrices.

[22] The LDFT formalism can be easily extended to arbitrary interactions $H_I = (1/2) \Sigma V_{ijkl} \hat{c}_{i\sigma}^\dagger \hat{c}_{k\sigma'}^\dagger \hat{c}_{l\sigma'} \hat{c}_{j\sigma}$, by replacing $U \Sigma_i \hat{n}_{i\uparrow} \hat{n}_{i\downarrow}$ by H_I in the expressions for the interaction-energy functional $W[\gamma]$. However, note that the functional $W[\gamma]$ depends crucially on the form of V_{ijkl}. See also Refs. 16 and 18.

[23] L.H. Lieb and F.Y. Wu, Phys. Rev. Lett. **20**, 1445 (1968); H. Shiba, Phys. Rev. B **6**, 930 (1972).

[24] For simplicity we focus here on bipartite lattices choosing $\gamma_{12} > 0$ and $t_{ij} = -t < 0$ for NN ij. Nonbipartite lattices can be treated analogously by considering positive and negative domains of γ_{12} separately, positive (negative) γ_{12} being relevant for negative (positive) values of the hopping integrals t_{ij} [see Eq. (1)]. As shown in Ref. 16, the scaling behavior of W/E_{HF} as a function of $g_{12} = (\gamma_{12} - \gamma_{12}^{\infty-})/(\gamma_{12}^{0-} - \gamma_{12}^{\infty-})$ is also observed for $\gamma_{12}^{0-} \leq \gamma_{12} \leq \gamma_{12}^{\infty-} \leq 0$. A similar situation occurs in dimerized systems where the domain of representability $[\gamma^\infty(\phi), \gamma^0(\phi)]$ depends on the ratio γ_{12}/γ_{23} between the bond orders corresponding to short and long bonds [$\phi = \arctan(\gamma_{12}/\gamma_{23})$, see Ref. 18].

[25] M. Takahashi, J. Phys. C **10**, 1289 (1977).

[26] N. Furukawa and M. Imada, J. Phys. Soc. Jpn. **60**, 3604 (1991); **61**, 3331 (1992).

[27] J.E. Hirsch, Phys. Rev. B **35**, 1851 (1987).

[28] Concerning the computational efficiency of LDFT, one may notice that the determination of E_{gs}, γ_{ij}^{gs}, and other derived properties involves very simply analytical expressions which correspond to the minimization of $E = E_K + W$ with respect to γ_{ij} [see Eq. (9)]. In the case of periodic systems these can be solved straightforwardly for any value of U/t and n. Most of the actually modest calculation effort goes in the determination of the functionals $W^{(2)}$ or $W^{(4)}$. This requires calculating γ_{12}^0 and γ_{12}^∞ only once for each system in order to define the domain of representability of γ_{12}. These preliminary calculations, as well as the number of variables involved in the minimization of E, become of course increasingly important as the symmetry of the systems is lowered (see, for example, Ref. 18).

[29] M.A. Ojeda, J. Dorantes-Dávila, and G.M. Pastor, Phys. Rev. B **60**, 6121 (1999); **60**, 9122 (1999).

[30] Y. Nagaoka, Solid State Commun. **3**, 409 (1965); D. J. Thouless, Proc. Phys. Soc. London **86**, 893 (1965); Y. Nagaoka, Phys. Rev. **147**, 392 (1966); H. Tasaki, Phys. Rev. B **40**, 9192 (1989).